

Material Modeling for Shape Deposition Manufacturing of Biomimetic Components

Xiaorong Xu¹, Wendy Cheng¹, Daniel Dudek², Mark R. Cutkosky¹, Robert J. Full², and Motohide Hatanaka¹

¹Stanford University, Bldg. 560, Panama Mall, Stanford, CA 94305, 650-723-4258, chengw@stanford.edu

²University of California at Berkeley, Dept. of Integrative Biology; Berkeley, CA 94720

ABSTRACT

As our understanding of the principles underlying animal locomotion improves, we are inspired to apply them to robot design. This has traditionally been achieved through controls or discrete mechanical devices; however, new manufacturing methods, such as Shape Deposition Manufacturing (SDM), offer us the opportunity to develop mechanisms containing intrinsic mechanical properties tailored for function. To properly utilize SDM, we must develop a bridge between biology and design. As a first step, we have conducted relaxation and dynamic tests on the ablated metathoracic limb of the *Blaberus discoidalis* cockroach and derived measures of stiffness and damping. We then tested an SDM-compatible polymer with similar viscoelastic properties. Comparison and understanding of the mapping between these two materials enables us to design and manufacture legs with stiffness and damping similar to those found in insects.

Keywords: biomimetic robotics, insects, viscoelastic materials, graded materials, shape deposition manufacturing (SDM).

NOMENCLATURE

B	geometric constant associated with relaxation analysis
C	damping constant
E	modulus of elasticity
G	shear modulus
I	moment of inertia
K_{leg}	stiffness of a leg
K_{rel}	stiffness normalized by weight
L_{joint}	moment arm for torsion
L	characteristic length

M	moment
l	moment arm
m	mass
Δ	phase shift between force and displacement
θ	angular displacement in time domain
τ	time constant equal to μ/E_1
$()_0$	amplitude or initial value
$()_1$	transient part of modulus/stiffness
$()_2$	storage part of modulus/stiffness
$()_r$	quantity associated with relaxation experiments
$()'$	dynamic storage modulus
$()''$	dynamic loss modulus
$()^*$	complex conjugate

INTRODUCTION

Materials found in Nature differ significantly from those found in human-made devices. Nature appears to design for “bending without breaking” and employs tissues that are compliant and viscoelastic [Vogel, 1995] rather than stiff, homogeneous, and isotropic. Even “stiff” natural materials, such as the calcified shells of crabs, have local areas that bend, buckle and bulge during motion [Blickhan *et al.*, 1993]. In addition, local variations in biological materials, tailored to meet local variations in loading, are common.

The nonlinear, compliant, and inhomogeneous materials found in even the simplest animals provide them with a sophistication and robustness that today's robots cannot match. However, as our ability to analyze and fabricate mechanisms with compliant and functionally-graded materials improves, we

have the opportunity to develop robots whose structures draw inspiration from simple animals such as insects and crustaceans.

One fertile area for biomimetic design is the legs of walking or hopping robots, where leg compliance has been recognized as especially important [Raibert, 1986]. Biologists studying subjects ranging from mammals to arthropods have also shown that natural legs are carefully designed and tuned for passive compliance. The deathhead cockroach (*Blaberus discoidalis*) possesses legs with compliant muscles and skeletal components that increase dynamic stability and disturbance rejection [Full and Koditschek, 1999] [Kubow and Full, 1999] [Meijer and Full, *in press*]. Leg compliance also varies dynamically. Running animals adjust the overall compliance of their legs to decrease impact forces and minimize energy costs [Alexander, 1990] while humans adjust their leg compliance to accommodate changes in surface hardness, stride frequency, mass, and leg inertia [Ferris *et al.*, 1998] [Farley *et al.*, 1998] [Farley and Gonzalez, 1996] [Obusek *et al.*, 1995].

For mobile robots to approach the speed and robustness of legged animals, we are inspired to reproduce some of the critical mechanical parameters found in natural legs. These characteristics – such as compliance – have traditionally been achieved through either sensing and control algorithms or discrete mechanical devices such as coil springs and pneumatic cylinders. However, inherent advantages exist in producing these parameters through mechanisms with intrinsic properties and local variations tailored for locomotion; with this approach, we can simplify controls and fabricate robots possessing robustness and speed closer to those of simple animals.

One method for manufacturing such robots is Shape Deposition Manufacturing (SDM), a rapid prototyping technology [Merz *et al.*, 1994]. SDM addresses many limitations of traditional manufacturing and assembly by enabling the *in situ* fabrication of mechanisms with complex geometry and heterogeneous materials [Binnard, 1999][Cham *et al.*, 1999][Bailey *et al.*, 1999].

Design and fabrication of layered and heterogeneous materials (also called Functionally Graded Materials - FGMs) has recently been a focus of research [Fessler *et al.*, 1997]. FGMs enable us to control local variations of biomimetic components by selectively depositing soft and hard materials.

To produce biologically inspired components of biomimetic mechanical properties, a bridge between biological findings and SDM design specifications is needed. The first requirement is to characterize biological structures and translate the characteristics into quantitative specifications for mobile robots. The second requirement is to model SDM material behavior to facilitate component design to meet these specifications.

To address these requirements we first performed experiments on a hind leg of *Blaberus discoidalis* and described its response to both step displacement inputs and sinusoidal

displacement excitations. Next, we tested one of the materials used in SDM, a soft polyurethane polymer largely used as joint material in manufacture, and fit the results to standard viscoelastic materials and models. Comparison and understanding of the mapping between these two studies enable us to begin to design and manufacture legs similar to those found in biology.

BIOLOGICAL CHARACTERIZATION

The cockroach legs and urethane polymers are both composed of long molecular chains. These chains move with respect to each other during macroscopic deformation, causing the material to exhibit viscoelastic behavior such as stress relaxation, creep, unrecoverable deformation, and hysteresis.

To obtain specific viscoelastic measures of standard materials, creep, relaxation, or dynamic experiments are performed and the results fit to the Maxwell, Voigt, or Standard Linear Solid models (Fig. 1). Researchers have also used these models to fit biological materials such as human bones and rabbit skin [Lakes, 1979a] [Lakes, 1979b] [Fung, 1994].

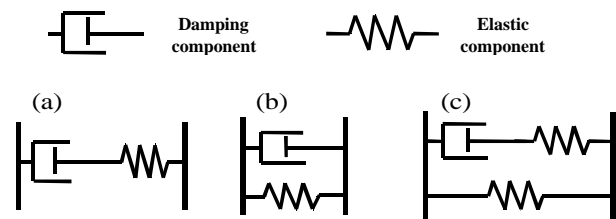


Figure 1. Viscoelastic models. (a) Maxwell model, (b) Voigt model, and (c) standard linear model.

Experiment Setup and Results

Relaxation and dynamic experiments were carried out on the hind leg of *Blaberus discoidalis* to aid in the selection of a material behavior model and to quantify measures of roach leg response (Fig. 2). During testing, the coxa of the ablated metathoracic limb (hind limb) of the cockroach was epoxied to 3/8" acrylic such that the coxa-femur and femur-tibia joints were free to rotate. Cyanoacrylate was used to attach one end of a stainless steel pin to the distal tip of the tibia; dental impression compound (Kerr) was used to adhere the other end of the pin to the arm of a servo-motor system (Aurora Scientific Dual-Mode Lever Arm System 300B-LR). The leg was then displaced with the Aurora system.

The Aurora system is based upon a high performance rotary moving coil motor supported by precision ball bearings. The motor is coupled with a capacitive position detector, and so can measure force and displacement simultaneously. We used this system to impose step displacements (with finite rise time) and sinusoidal excitations on the leg, then monitored resulting forces. We estimate the total error in the force-displacement measurements to be less than 4 %.

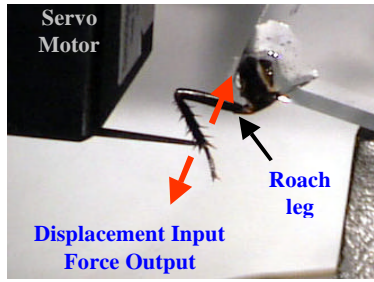


Figure 2. *Blaberus* hind leg test setup.

The cockroach leg was displaced in a direction orthogonal to the joint motion at amplitudes 0.3 mm, 0.7 mm, and 1.0 mm. These values were chosen since observations of locomoting *Blaberus* showed that the deflection of the hind leg in this direction was less than 1.0 mm. Step inputs at these amplitudes produced relaxation curves where the reaction forces initially peaked and then attenuated to constant force levels (Fig. 3).

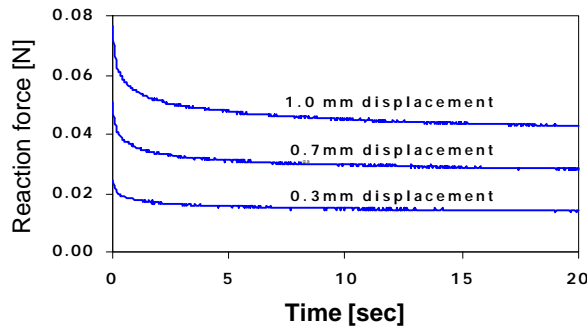


Figure 3. Force relaxation histories of *Blaberus* leg with step displacement inputs at three amplitudes.

Dynamic tests with sinusoidal displacement inputs ranging in frequency from 0.01 Hz to 100 Hz were performed. The *Blaberus* has a preferred trotting frequency of approximately 12 Hz, at which it behaves similar to an inverted spring/pendulum [Full and Tu, 1990] [Blickhan and Full, 1993]. Figure 4 shows the force-displacement profile at 0.02 Hz, 12 Hz, and 50 Hz vibration frequencies and 0.5 mm deflection amplitude. At lower frequencies and smaller amplitudes, the response hysteresis curve approached that of a standard viscoelastic solid. As the frequency and amplitude increased, the response grew increasingly nonlinear such that, at vibration frequency greater than 40 Hz, the curve became skewed. Therefore, some of the data such as phase angle are calculated only for frequencies equal to or lower than 40 Hz. In addition, some of the force-displacement plots are not centered about zero-zero due to an initial negative force offset present during the trials.

Associated with this hysteresis curve is a phase shift in which the measured output force leads the input displacement. This phase shift is similar to the ‘loss angle’ in viscoelastic materials. Figure 5 plots the phase shift for vibration frequencies between 0.01 Hz and 50 Hz, where the hysteresis curve approximates

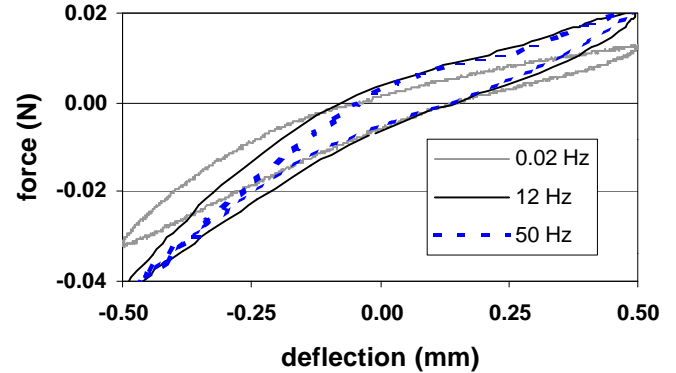


Figure 4. *Blaberus* leg force response to sinusoidal displacements at 0.02, 12, and 50 Hz and -0.5 to 0.5 mm.

that of a viscoelastic solid. At low frequencies, an average stiffness of 45 N/m can be directly read from the plots by taking the slope of the line connecting the tips of the force-displacement loops [Blickhan, 1986].

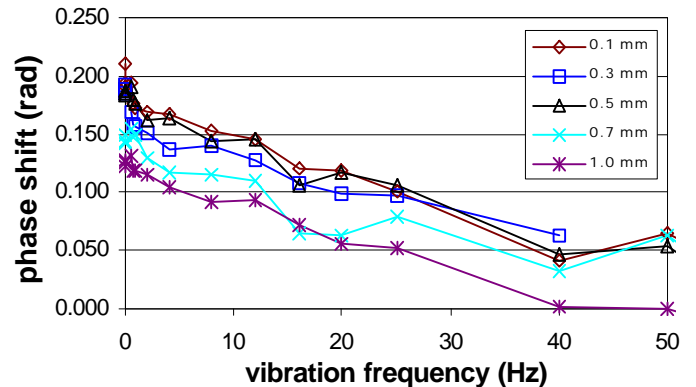


Figure 5. Phase shift (force leads displacement) from sinusoidal displacement inputs.

Model of cockroach leg

The results of these tests indicate that a cockroach leg excited in a direction orthogonal to the joint direction behaves similarly to a viscoelastic material. The exponential nature of the force relaxation curves suggests viscoelasticity. The hysteretic nature of the force-displacement curves indicates that there is energy loss due to the internal friction, which is a common characteristic for viscoelastic materials.

The cockroach leg is subject to a combination of bending and torsion in the experiment. The overall effect can be modeled as a torsion spring with a moment arm (Fig. 6). Additional assumptions for the model include: (1) the axis of rotation for the leg is constant during torsion and (2) the joint material can be approximated using a lumped-parameter element with uniformly distributed linear viscoelastic properties.

Model of relaxation test results. With this simplification, the relaxation test results imply that the step response of a

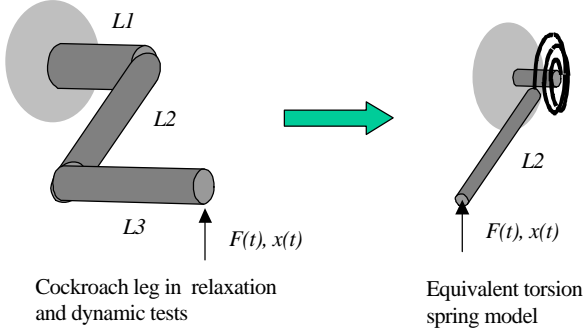


Figure 6. Model of the cockroach leg as a torsion spring with a moment arm.

cockroach leg under a constant rotation angle can be mathematically described by:

$$M_r(t) = B\theta_0(G_2 + G_1e^{-t/\tau_r}) \quad (1)$$

Where $M_r(t)$ is the reaction moment relaxation history due to the step angular input θ_0 , B is a constant associated with the leg and joint geometry, G_1 is the transient part of the shear modulus, and G_2 is the equilibrium shear modulus after infinite time.

Since torsion is mainly caused force at the tibia tip, Eq. (1) can be rewritten as a relation between force and displacement:

$$f_r(t) = \frac{Ba_0}{l^2}(G_2 + G_1e^{-t/\tau_r}) \quad (2)$$

Where $f_r(t)$ is the reaction force recorded in the relaxation experiment, a_0 is the amplitude of the sinusoid deflection, and l is the arm of the moment.

Equation (2) can be solved for BG_1 and BG_2 by considering the cases of $t = 0$ and as t approaches infinity:

$$BG_1 = \frac{l^2}{a_0}[f(0) - f(\infty)] \text{ and } BG_2 = \frac{l^2}{a_0}f(\infty) \quad (3)$$

By plugging the force-displacement relation (Eq. (2)) into the cockroach leg relaxation data (Fig. 3), one can obtain the time constant τ_r as 1.92 seconds. The exponential expression of the shear modulus is not available since the geometric factor B is unknown. However, we can derive that $BG_1 = 3.38 \times 10^{-3} (Nm)$ and $BG_2 = 3.17 \times 10^{-3} (Nm)$ with standard deviations of $0.15 \times 10^{-3} (Nm)$ and $0.30 \times 10^{-3} (Nm)$, respectively.

Correlation with Standard Linear Model. The experiments on the cockroach leg can be modelled from a linear perspective as shown in Fig. 7. The force and displacement relation in the frequency domain for this system is:

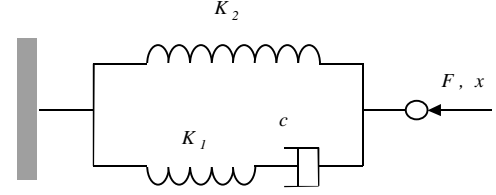


Figure 7. Macroscopic model of cockroach leg used for analysis of displacement step response.

$$\frac{F(s)}{X(s)} = \frac{C(K_1 + K_2)s + K_1K_2}{Cs + K_1} \quad (4)$$

By comparing the step response predicted by this model with Eq. (2), one can obtain simple expressions of the stiffness and damping parameters from the viscoelastic property data.

$$K_1 = \frac{BG_1}{l^2}, K_2 = \frac{BG_2}{l^2}, \text{ and } C = \frac{BG_1}{l^2}\tau_r \quad (5)$$

For the cockroach leg tested, $K_1 = 34 \text{ N/m}$, $K_2 = 43 \text{ N/m}$ and $C = 65 \text{ Ns/m}$. With K_1 , K_2 and C , one can predict the force relaxation history as shown in Fig. 8.

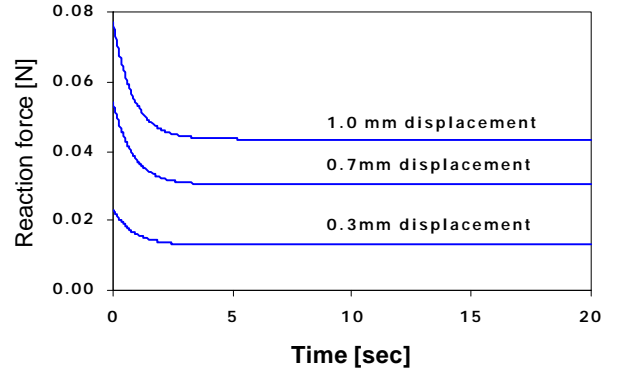


Figure 8. Predicted relaxation history (compare with Fig. 3.)

Comparison of Fig. 3 and Fig. 8 shows that, for displacements of 0.3, 0.7, and 1.0 mm, experimental results differ from modeling results by approximately -7.6 %, 6.8 % and 0.1 %, respectively. The corresponding standard deviations are 5.1 %, 5.9 %, and 5.4 %, respectively.

Model of sinusoidal excitation test results. The torsion spring representation of the cockroach leg can also be applied to analyze the dynamic response of the leg. The force response results from the reaction moment of the material and the moment associated with the inertia of the leg and steel pin.

$$M_e = G^*k\theta + I\frac{d^2\theta}{dt^2} \quad (6)$$

Where G^* is the complex form of the dynamic modulus combining G' , the dynamic storage modulus, and G'' , the dynamic loss modulus.

$$G^* = G' + G''i \quad (7)$$

The sinusoid angular input in complex form is:

$$\theta = \theta_0 e^{i\omega t} \quad (8)$$

The dynamic response of the cockroach leg in the complex form is therefore:

$$f(t) = \frac{a_0}{l^2} e^{i\omega t} [(BG' - I\omega^2) + BG''i] \quad (9)$$

Where ω is the angular velocity of the vibration and a_0 is the amplitude of the vibration.

Similar to the force relaxation case, results from the dynamic experiment can not yield exact expressions of material shear moduli, but rather with a geometric factor B :

$$BG' = I\omega^2 + \frac{F_0 l^2}{a_0 \sqrt{1 + (\tan \Delta)^2}}, \text{ and } BG'' = \frac{F_0 l^2 \tan \Delta}{a_0 \sqrt{1 + (\tan \Delta)^2}} \quad (10)$$

Where Δ is the phase shift (loss angle) of the force versus the displacement, F_0 is the amplitude of the force (i.e., applied force minus inertia force), and l is the length of the moment arm for the input force. Application of the above expressions to the dynamic test data yields the dynamic storage and loss moduli (multiplied by the geometric factor) as functions of the vibration frequency and amplitude.

Correlation with Voigt model. The simplest linear model that can be used to fit the dynamic response data is the Voigt model. Experimental results show that the input displacement (x) and the output force (f) differ mainly in magnitude and a phase shift (Δ). Mathematically, they can be described by:

$$x(t) = X_0 \cos(\omega t) \text{ and } f(t) = F_0 \cos(\omega t + \Delta) \quad (11)$$

Taking the Laplace transform of Eq. (11) and solving for the transfer function $F(s)/X(s)$ yields:

$$\frac{F(s)}{X(s)} = \frac{F_0}{X_0} \left(\frac{\sin(\Delta)}{\omega} s + \cos(\Delta) \right) \quad (12)$$

This transfer function is similar to that of a system consisting of a spring of stiffness K in parallel with a damper with damping constant C (Fig. 9).

$$\frac{F(s)}{X(s)} = Cs + K \quad (13)$$

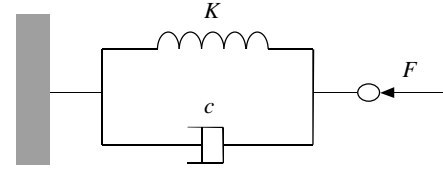


Figure 9. Macroscopic model of cockroach leg used in analysis of sinusoidal displacement response.

In the above model, K and C can be obtained from the material property parameters BG' and BG'' :

$$K = \frac{BG'}{l^2} \text{ and } C = \frac{BG''}{\omega l^2} \quad (14)$$

Since BG' and BG'' vary with the vibration frequency, the resulting K and C are also functions of the frequency. Fig. 10 predicts the damping constant according to Eq. (14). It is shown from the figure that the damping decreases as the vibration frequency increases.

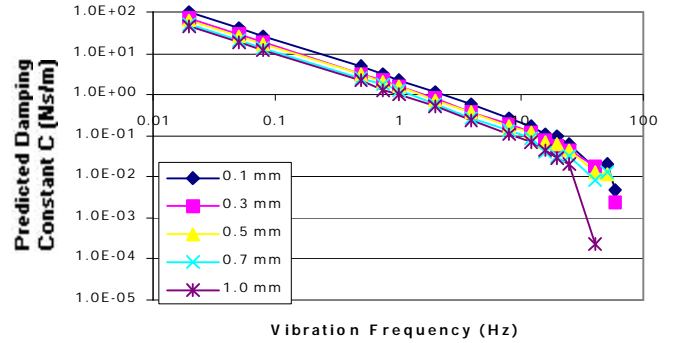


Figure 10. Predicted damping constant as a function of frequency.

The K and C values obtained from Eq. (14) can be further used to produce force-displacement hysteresis loops and visually compared with experiment data (Fig. 11). The model appears good for low frequencies and small amplitudes of vibration, when the cockroach leg behaves in a linear viscoelastic manner. For frequencies higher than 40 Hz or frequencies higher than 16 to 20 Hz at deflection amplitudes of 0.7 and 1.0 mm, the fit degrades noticeably. This is largely due to the nonlinear nature of the leg response at these vibration values.

The model can also be evaluated quantitatively. Comparison of the predicted and measured K show that they are extremely close; the predictions are lower than measured values by an average of 1%, with a standard deviation of 0.6%.

The energy loss for the viscoelastic material is caused by the internal friction of the material. It is represented by the area within the ellipse of stress vs. strain in dynamic loading. With the stiffness K and damping constant C obtained before, we are able to calculate the energy dissipation per cycle for different frequencies and compared with the experimental measurement.

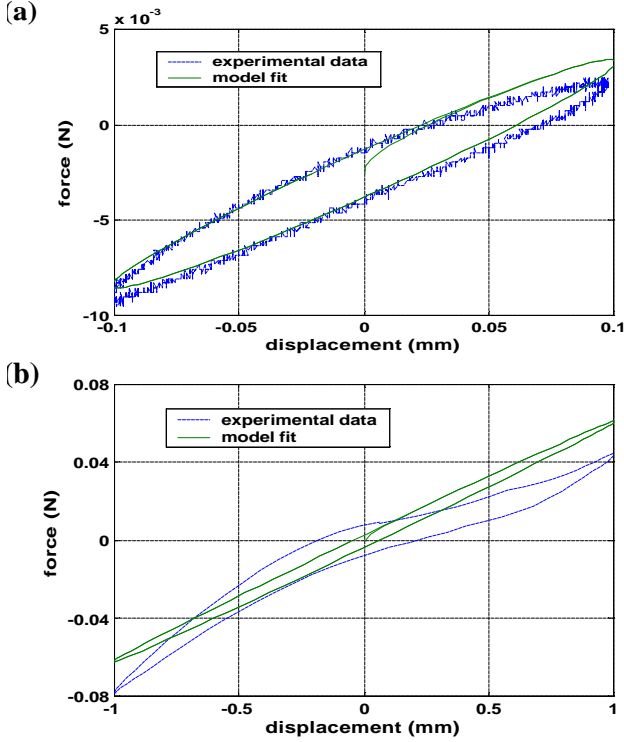


Figure 11. Comparison of experimental data and Voigt model. (a) 0.1 mm and 0.02 Hz, (b) 1.0 mm and 40 Hz.

Figure 12 plots the deviation between predicted and measured energy loss per cycle. The analysis shows that the C predictions were more accurate at smaller amplitudes and lower frequencies. For vibration amplitudes of 0.1 mm, 0.3 mm, and 0.5 mm, the average difference was 6% to 10%. For the 0.7 mm and 1.0 mm amplitudes, the difference averaged 30% to 40%.

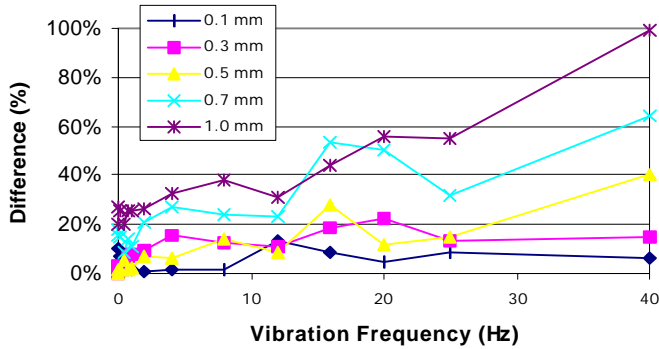


Figure 12. Deviation between predicted (Voigt model) and measured energy loss per cycle.

Evaluation of Model Fit

The lumped-parameter torsional model of the cockroach leg appears to be adequate as an estimation of the behavior of the cockroach leg at the range of amplitudes studied (from 0.1 mm to 1.0 mm) and at frequencies of less than 40 Hz. For higher frequencies, the cockroach leg deviates significantly from the linear viscoelastic behavior predicted by these models.

Linkage between relaxation and sinusoidal results

The models shown in Fig. 7 and Fig. 9 are reminiscent of the standard linear solid and the Voigt material models of viscoelastic behavior (Fig. 1). The material properties derived, BG_1 , BG_2 , BG' , and BG'' , (the scaled loss modulus, storage modulus, dynamic storage modulus, and dynamic loss modulus, respectively) are also very similar to the material constants associated with the standard linear solid model. This motivates us to find a constitutive law for the cockroach leg material that accounts for both the relaxation and sinusoid results.

In linear viscoelastic theory, the Boltzmann superposition integral is used to express dynamic stress history [Lakes, 1999]:

$$\sigma(t) = \int_{-\infty}^t E(t-\tau) \frac{d\varepsilon}{d\tau} d\tau = (E' + iE'')\varepsilon(t) \quad (15)$$

Combining the Boltzmann superposition integral with linear viscoelastic theory enables us to create a link between the constitutive measures G_1 and G_2 and the dynamic measures G' and G'' . If the standard linear solid model is used, BG' and BG'' , the dynamic storage and loss moduli for sinusoidal shear strain input, can be written in terms of the shear moduli, BG_1 and BG_2 : [Lakes, 1999]

$$BG' = BG_2 + \frac{\omega^2 \tau^2}{1 + \omega^2 \tau^2} BG_1, \text{ and } BG'' = \frac{\omega \tau}{1 + \omega^2 \tau^2} BG_1 \quad (16)$$

Figure 13 plots the predicted BG' and BG'' moduli calculated from the values of BG_1 and BG_2 . For comparison, BG' and BG'' calculated directly from experimental data (Eq. (10)) at an amplitude of 0.3 mm are also plotted.

These plots show that the standard linear solid model is good to build a linkage between BG_1 , BG_2 , and the dynamic storage modulus BG' . However the dynamic loss modulus BG'' can not be well predicted by a standard linear solid model. This indicates that the properties of viscoelastic material are too complex to be properly modeled by a simple constitutive law. Similar observations were documented for other viscoelastic materials [Ferry, 1970] as well as prior experiments with human cortical bone [Lakes, 1979].

The major contradiction between the commonly used linear viscoelastic model and the biological material test for biological materials is that the former predicts a phase shift that decreases to zero as the frequency of excitation decreases. However, this was not true for a cockroach leg excited in a direction orthogonal to joint movement (Fig. 5). The phase shift (or loss angle) is the lag of the strain with respect to stress in a dynamic loading. It is defined as a function of BG' and BG'' :

$$\Delta = \arctan\left(\frac{BG''}{BG'}\right) = \arctan\left(\frac{BG''}{BG'}\right) \quad (17)$$

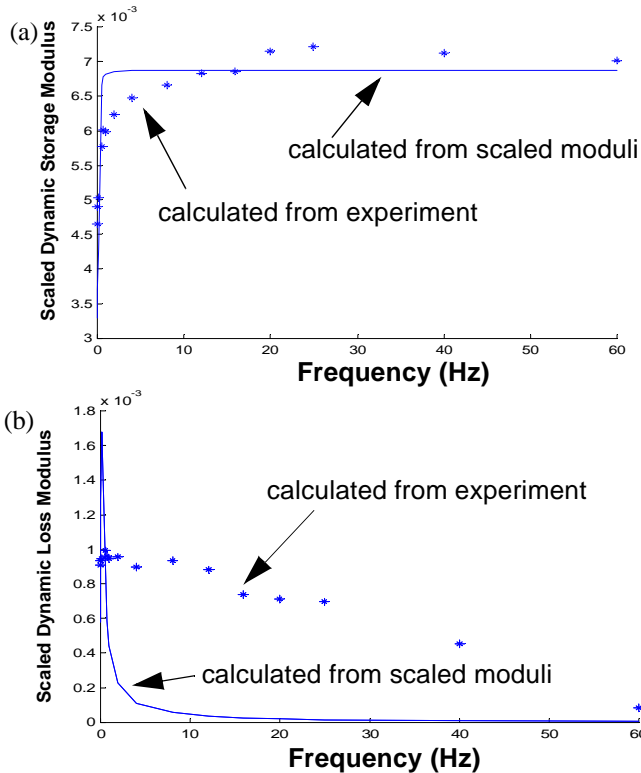


Figure 13. Scaled moduli calculated from BG_1 and BG_2 and from the experiment: (a) dynamic storage modulus (BG'), (b) dynamic loss modulus (BG'').

The phase shift significantly affects the shape of the hysteresis curve and, thus, the energy dissipation. In the cockroach leg experiment, the energy dissipation at low frequency is observed to be high, while that for a typical linear viscoelastic model is low. Adaptations of the linear viscoelastic model may yield a better representation of the behavior of materials such as the cockroach leg. With better understanding of how the material characteristics BG_1 , BG_2 , BG' , and BG'' relate to each other, we will better understand and characterize the behavior of biological components such as the cockroach leg.

SDM MATERIAL CHARACTERIZATION

The SDM process offers us the opportunity to integrate a range of desired impedance into the structure of robot legs for improved robustness and simpler control. SDM-compatible materials span a wide range of material properties and the SDM process enables us to control local variations through Functionally Graded Materials (FGM) [Suresh, 1998].

Figure 14 shows a SDMed 5-bar linkage containing FGM. The linkage combines two polyurethanes geometrically to form links and joints. Although its morphology does not mimic that of a leg, this 5-bar linkage can be scaled to obtain comparable compliance and damping properties. Such scaling requires material property information beyond what the manufacturer can provide, and these SDM materials must be characterized.

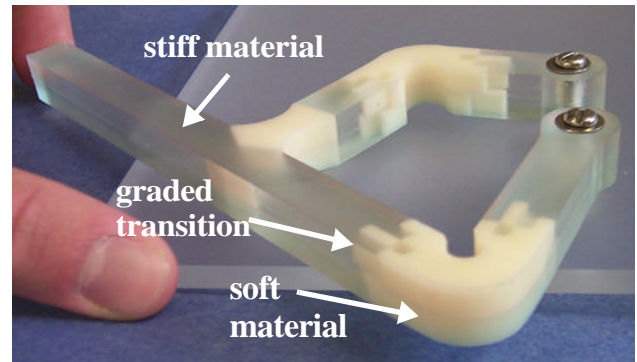


Figure 14. A 5-bar linkage exploiting functionally graded materials to control local compliance and damping. The joints of the 5-bar are fabricated from polyurethane (Innovative Polymer's IE-90A.)

We have developed a dynamic testing machine (Fig. 15) for this purpose. This testing machine is based on a voice coil actuator; the machine controls force input and measures subsequent displacement of the sample. The machine accepts multiple fixtures and can undertake various torsion, bending, and tension tests for sample sizes up to 12 cm x 12 cm x 5 cm. The actuator is driven by a current amplifier that translates voltage input from a signal generator to proportional current output. A 0.9 kg full bridge thin beam load cell coupled with a strain gauge processor for signal magnification and conditioning measures the actuating force; an LVDT measures the displacement of the actuator. Data from the load cell and the LVDT are collected via a LabView program and a National Instruments DAQ board.

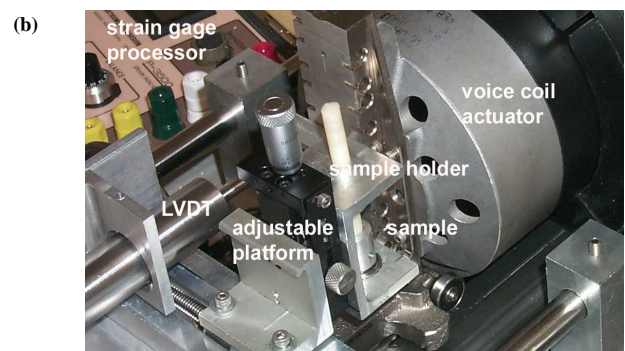
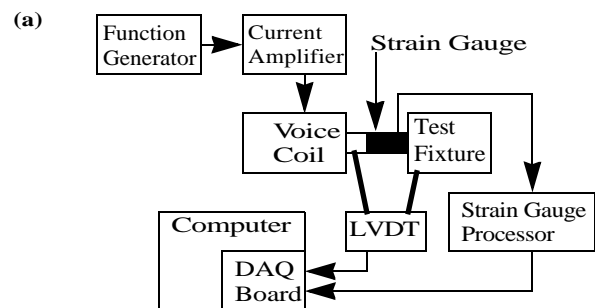


Figure 15. (a) Schematic drawing of test machine. (b) Close view of the test machine

Dynamic Tests for the SDM Material

We performed dynamic test measurements for IE-90A polyurethane (Innovative Polymers Inc.), the material of the soft joints in the FGM parts shown in Fig. 14. IE-90A cylindrical test samples were cast from resin and hardener mixed as per manufacturer's instructions and degassed in a vacuum chamber. The samples were of diameter 6.35 mm and length 63.5 mm and formed in a wax mold. After curing, the demolded sample was aged for 2 additional days prior to testing.

During testing, the sample was affixed between two coaxial holders spaced 21.6 mm apart. The upper end of the sample was held immobile on the fixture platform, while the lower end was seated within a bearing. The bearing was rotated via an extension arm attached to the voice coil actuator. Sample response to sinusoidal force inputs ranging from 0.2 Hz to 20 Hz at amplitudes of 0.5 mm and 1.0 mm were taken. Fig. 16a shows a typical hysteresis curve for IE-90A.

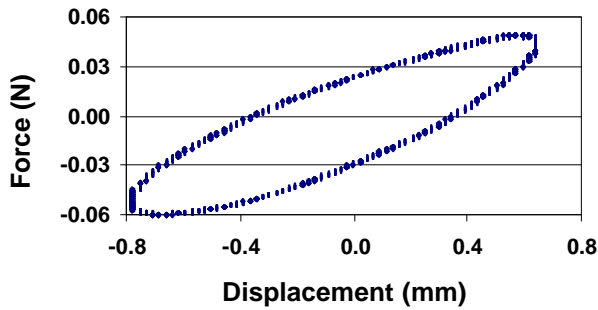


Figure 16. Typical hysteresis curves at 10 Hz with IE-90A rod sample.

The dynamic loss and storage moduli can then be calculated from the phase angle data obtained from experiment from a procedure similar to the cockroach leg analysis (Fig. 17.)

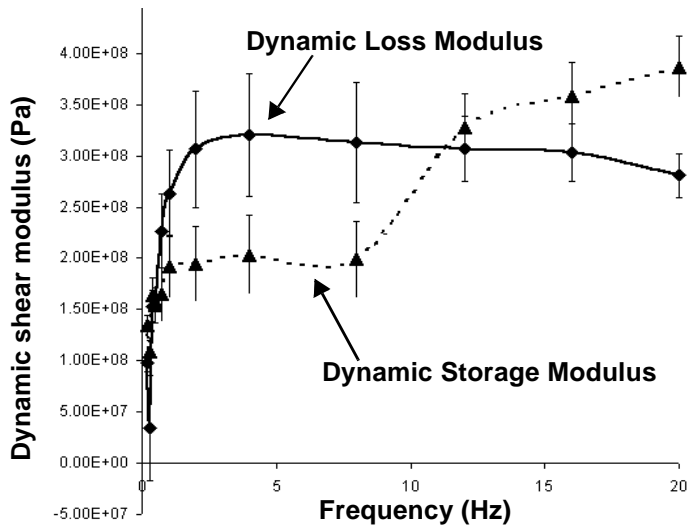


Figure 17. Dynamic storage G' and loss G'' moduli for the soft polymer material.

Sources of error include some inertia and compliance of the moving clamp and extension arm assembly (described by Eq. (6)) and the limited resolution of the DAQ system. We estimate the measurement error to be approximately 10 % of measured force at 20 Hz and lower at lower frequencies.

Variations not related to the test machine stem from nonlinear polyurethane material properties and manufacturing issues. While the geometry of SDM parts can be held to standard machining accuracy and repeatability [Rajagopalan, 2000], the mechanical properties of these parts vary more significantly. Factors such as variability in the age and material lot of resins and hardeners, exact mixing and pouring procedures, material defects introduced during machining, and exposure to moisture and UV light during curing play especially important roles. Innovative Polymers has not rigorously characterized variation between lots, but estimates 3 % to 8 % flexural modulus variation for polyurethanes stiffer than IE-90A (information about IE-90A is unavailable.) Quantitative measures of the effects of the other factors have yet to be performed¹.

Design of Biomimetic Legs

With information regarding the mechanical behavior of animal legs and the material characteristics of SDM materials, we can develop guidelines for biomimetic leg design. Previous research has demonstrated that most animals can be modelled as bouncing, spring-mass monopodes despite variations in leg number, leg length, position, and exoskeleton/endoskeleton. This is because the energetics and dynamics of trotting, running, and hopping animals are dynamically similar within the locomotion method [Blickhan and Full, 1993] [Blickhan, 1989].

For animals to utilize dynamically similar locomotion methods, the vertical stiffnesses (K_{rel} as expressed in Eq. (18)) across animals types must be relatively constant.

$$K_{rel} = \frac{F}{(mg)} \frac{\Delta L}{L} \quad (18)$$

Where L is a characteristic leg length determined by the leg length, the locomotion scheme, and the number of legs of the animal, F_v is the vertical force applied by the animal on the ground during midstance, and ΔL is the change in leg length that results from this vertical force. For trotters, the relative whole body stiffness K_{rel} ranges from 7.1 (turkey) to 25.6 (kangaroo rat) but averages around 18.6 [Blickhan and Full, 1993].

The vertical whole body stiffness at midstance for a specific animal is:

$$K = \frac{F}{\Delta L} = \frac{K_{rel}}{L} \quad (19)$$

1. Please see <http://www-cdr.stanford.edu/biomimetics> for additional information regarding SDM materials and SDM processing for biomimetics.

According to the viscoelastic model discussed previously, this leg stiffness can be expressed as a function of the complex dynamic modulus and the leg geometry:

$$K_{leg} = \frac{B|G^*|}{L^2} \quad (20)$$

Where B is a geometric factor, L is the characteristic leg length, and $|G^*|$ is the magnitude of the dynamic modulus that varies with respect to the vibration frequency.

Insects tend to run at their natural frequencies to maximize energy economy [Blickhan 1989]. This frequency can be estimated from the vertical stiffness obtained from the monopode model:

$$f = \frac{1}{2\pi} \sqrt{\frac{K}{m}} \quad (21)$$

Equation (18) through Equation (21) build a set of guidelines for relating animal size, characteristic leg length, leg stiffness, locomotion frequency, and leg material property for animals using similar locomotion methods. Let us consider these guidelines with respect to Nature's design on the *Blaberus discoidalis* leg. *Blaberus* is a trotter with body mass of approximately 0.003 kg. Geometric scaling against other trotters yields a virtual leg length of 0.02 m. These values enable us to estimate the vertical whole body stiffness and natural frequency as 25 N/m and 91 rad/sec (14 Hz), respectively. At this frequency, the linear viscoelastic model predicts a magnitude of B/G^* of 0.0069 Nm. Plugging this value into Eq. (20) yields a leg stiffness of 18 N/m.

For comparison, data from the cockroach used in calculating the monopode model constants yield an estimated vertical whole body stiffness closer to 32 N/m for that cockroach. If we assume that the vertical whole body stiffness of the *Blaberus* is evenly distributed among the three legs of a tripod, then the individual leg stiffness is approximately 11 N/m. This measured leg stiffness is similar to that of the predicted stiffness above. The differences largely result from approximations made in the monopode model and the dynamic modulus being obtained in a direction not exactly vertical to the ground at midstance.

Having reviewed these equations for the cockroach leg, let us attempt the design of a biomimetic leg. At present, the sizes of available motors, valves, and sensors limit us to crab-sized (vs. cockroach-sized) robots². For a trotting robot with target mass 0.26 kg and characteristic leg length of 100 mm, the monopode model predicts the vertical whole body stiffness as 430 N/m. If this robot is a hexapod walking machine with a tripod gait, the average stiffness per leg is approximately 140 N/m.

A very simple leg design might be a soft polyurethane rod with diameter D and length L_{joint} connected to a stiff linkage of length L . Then the desired L_{joint} is:

$$L_{joint} = \frac{\pi D^4 \cdot |G^*|}{32 L^2 \cdot K_{leg}} \quad (22)$$

Where $|G^*|$ is the magnitude of the dynamic modulus.

In order to find $|G^*|$, we must first estimate the locomotion frequency, which the monopode model predicts as 6.5 Hz. The $|G^*|$ value for the soft polyurethane material we characterized is about 4×10^8 Pa at that frequency. If we set the rod diameter to 3.2 mm, the required joint length L_{joint} is 4.8 mm.

The above example is only an exercise demonstrating a very simple case of leg design, and the resulting leg is biomimetic only with respect to general stiffness and damping, and not specific function. Functionally biomimetic legs are more complex to accommodate differing loading conditions, leg shapes, and joint geometry. Nevertheless, once the material properties of the fabrication materials are obtained, one can design the leg according to target functional values.

CONCLUSIONS

Some polymer materials that can be used in SDM are similar to the biological materials found in insect legs that exhibit viscoelasticity. This inspires us to develop material models and design methodologies that can be used to guide biomimetic robot leg design and material selection. In this paper, we have discussed a simple linear, lumped parameter model used to characterize cockroach leg behavior in relaxation experiments and in response to sinusoidal excitations. We have also developed a dynamic test machine and begun characterizing a polyurethane material used for SDM fabrication of robot joints.

Our current models of leg response assume linear viscoelasticity. The correlation between these models and the results of experiments is relatively good at low frequencies and small displacements, but deteriorates at higher frequencies and displacements as nonlinear effects grow pronounced. In addition, at very low frequencies, dynamic tests on cockroach legs indicate a higher loss modulus than that predicted by a standard linear model. Should these nonlinear aspects of leg behavior prove important for locomotion, we will need to develop better models to simulate the viscoelastic behavior of the leg in a wide frequency range.

To produce legs with mechanical response similar to that of the real cockroach leg, we need to better characterize additional SDM materials beyond what can be obtained from the manufacturer. Knowledge of SDM material behavior, along with information about the aspects of leg behavior important to locomotion, will enable us to draw general design guidelines for designing biomimetic legs.

2. The SDM process is capable of millimeter features (Cooper, *et al.*, 1998).

ACKNOWLEDGMENTS

The authors thank the members of the Stanford DML, Stanford RPL, and Berkeley PolyPEDAL teams for their contributions to the work documented in this paper. Wendy Cheng is supported by a combined NSF and Stanford Graduate Fellowship. This work is supported by the National Science Foundation under grant MIP9617994 and by the Office of Naval Research under N00014-98-1-0699.

REFERENCES

- Alexander, R. M., 1990, "3 uses for springs in legged locomotion," *Int. J. Robotics Research*, Vol. 9 (#2), pp. 53-61.
- Bailey, S. A.; Cham, J. G.; Cutkosky, M. R.; Full, R.J., 1999, "Biomimetic robotics mechanisms via shape deposition manufacturing," *9th Int. Symp. Robotics Research*, Snowbird, Utah, Oct. 9-12, 1999, p. 321-327.
- Binnard, M., 1999, "Design by composition for rapid prototyping," Ph.D. Dissertation, Stanford University, Stanford, CA.
- Blickhan, R., 1989, "The spring-mass model for running and hopping," *J. Biomechanics*, Vol. 22 (#11-1), pp. 1217-1227.
- Blickhan, R., 1986, "Stiffness of an arthropod leg joint," *J. Biomechanics*, Vol. 9 (#5), pp. 375-384.
- Blickhan, R. and Full, R.J., 1993, "Similarity in multilegged locomotion: bouncing like a monopode", *J. Comparative Physiology A*, Vol. 173 (#5), pp. 509-517.
- Cham, J.G.; Pruitt, B.L.; Cutkosky, M.R.; Binnard, M.; Weiss, L.E.; Neplotnik, G., 1999, "Layered manufacturing with embedded components: process planning issues," *ASME Proc. DETC '99*. Las Vegas, Nevada. September 12-15.
- Cooper, A.G.; Kang, S.; Kietzman, J.W.; Prinz, F.B.; Lombardi, J.L.; Weiss, L., 1998, "Automated fabrication of complex molded parts using mold SDM," *Proc. Solid Freeform Fab. Symp.*, UT Austin, Texas, August 8-10.
- Farley, C.T. and Gonzales, O., 1996, "Leg stiffness and stride frequency in human running," *J. Biomechanics*, Vol. 29 (#2), pp. 181-186.
- Farley, C.T.; Houdijk, H.H.P., Vanstrien, C., and Louie, M., 1998, "Mechanism of leg stiffness adjustment for hopping on surfaces of different stiffness," *J. Applied Physiology*, Vol. 85 (#3), pp. 1044-1055.
- Ferris D.P.; Louie M.; Farley C.R., 1998, "Running in the real-world: adjusting leg stiffness for different surfaces," *Proceeding of the Royal Society of London Series B - Biological Sciences*, Vol. 265 (#1400), pp. 989-994.
- Ferry, J.D., *Viscoelastic Properties of Polymers*, 1970, John Wiley & Sons, New York.
- Fessler J.; Nickel, A.; Link, G.; Prinz, F.; Fussel, P., 1997, "Functional gradient metallic prototypes through shape deposition manufacturing," *Proc. Solid Freeform Fabrication Symp.* Austin, TX, September, 1997, pp. 521-528
- Full, R.J. and Koditschek, D. E., 1999, "Templates and Anchors - Neuromechanical hypotheses of legged locomotion on land," *J. Experimental Biology*, Vol. 202, pp. 3325-3332.
- Full, R.J. and Tu, M.S., 1990, "The mechanics of 6-legged runners," *J. Experimental Biology*, Vol. 148, pp. 129-146.
- Fung, Y.C., 1994, "Chapter 7: Bioviscoelastic Solid" in *Biomechanics: Mechanical Properties of Living Tissues*.
- Kubow, T.M. and Full, R.J., 1999, "The role of the mechanical system in control: a hypothesis of self-stabilization in hexapedal runners," *Philosophical Transactions of the Royal Society of London B*, Vol. 354, pp. 849-862.
- Lakes, R.S.; 1999. *Viscoelastic Solids*, CRC press, Boca Raton.
- Lakes, R. S.; Katz, J. L.; Sternsterin, S.S., 1979a, "Viscoelastic properties of wet cortical bone 1: torsional and biaxial studies," *J. Biomechanics*, Vol. 12 (#9), pp. 657-678.
- Lakes, R. S.; Katz, J. L.; Sternsterin, S.S., 1979b, "Viscoelastic properties of wet cortical bone 1: relaxation mechanisms," *J. Biomechanics*, Vol. 12 (#9), pp. 679-687.
- Meijer, K. and Full, R. J., "Stabilizing properties of invertebrate skeletal muscle." *American Zoologist*. In press.
- Merz, R.; Prinz, F.B.; Ramaswami, K.; Terk, M.; Weiss, L., 1994, "Shape deposition manufacturing," *Proc. Solid Freeform Fabrication Symp.* University of Texas at Austin, August 8-10.
- Obusek, J; Holt, K; Rosenstein, R, "The hybrid mass-spring pendulum model of human leg swinging: stiffness in the control of cycle period", *Biological Cybernetics*, Vol. 73, pp. 139 1995.
- Raibert, M.H., 1986, *Legged Robots that Balance*, MIT Press, Cambridge, MA.
- Rajagopalan, S., 2000, "Error Analysis for the In-Situ Fabrication of Mechanisms," accepted *Proc. DETC/DTM*, Baltimore, MD, Sept. 10-13.
- Suresh, S. and Mortenen, A., 1998. *Fundamentals of Functionally Graded Materials*, IOM Communications Ltd, London, U.K.
- Vogel, S., 1995, "Better Bent Than Broken", *Discover*, Vol. 16, No. 5, pp 62.